In presenting the dissertation as a partial fulfillment of the requirements for an advanced degree from the Georgia Institute of Technology, I agree that the Library of the Institution shall make it available for inspection and circulation in accordance with its regulations governing materials of this type. I agree that permission to copy from, or to publish from, this dissertation may be granted by the professor under whose direction it was written, or, in his absence, by the dean of the Graduate Division when such copying or publication is solely for scholarly purposes and does not involve potential financial gain. It is understood that any copying from, or publication of, this dissertation which involves potential financial gain will not be allowed without written permission.

_____ _____

VAPOR CAVITY FORMATION IN A PIPE AFTER VALVE CLOSURE

A THESIS

Presented to

the Faculty of the Graduate Division

by

William E. Heath

In Partial Fulfillment

of the Requirements for the Degree

Master of Science in Civil Engineering

Georgia Institute of Technology

September, 1962

VAPOR CAVITY FORMATION IN A PIPE

AFTER VALVE CLOSURE

Approved:

Date Approved by Chairman: March 20, 1963

ACKNOWLEDGMENTS

The writer wishes to thank all persons who made this thesis possible. Dr. M. R. Carstens was the thesis advisor, and the guidance given by him is greatly appreciated. The other members of the reading committee were Prof. C. E. Kindsvater and Dr. P. H. Sanders.

Mr. Homer J. Bates, laboratory technician, assisted in the construction of the experimental equipment. The writer also wishes to thank Mr. C. S. Martin, who helped with the mathematics in the derivation of the equations.

The experimental apparatus is to become part of the permanent equipment in the Hydraulics Laboratory. The writer is grateful to the School of Civil Engineering for their financial aid in the construction of this equipment.

TABLE OF CONTENTS

LIST OF FIGURES

NOMENCLATURE

A	area of pipe in ft^2
C	circumference of inside of pipe in ft
D	diameter of pipe in ft
Ep	modulus of elasticity of pipe material in psf
Ew	bulk modulus of elasticity of water in psf
J_o	Bessel coefficient of order zero
J_1	Bessel coefficient of order one
L	length of pipe in ft
P	pressure gradient in ft/sec
P'	dimensionless pressure parameter = $\frac{Pa^2}{V_o}$
Q	discharge in cfs
R	Reynolds Number
U_o	pipe velocity at t = 0 in fps
V	mean pipe velocity in fps
V_o	steady-flow velocity existing before valve closure in fps
V'	dimensionless velocity parameter = V/V_o
a	radius of pipe in ft
c	celerity of sound in water in fps
p	piezometric pressure at the valve in psf
$\triangle$ p	pressure drop from the reservoir to the valve in psf
p_a	piezometric pressure at the valve immediately before the compression shock wave is generated in psf
p_o	static pressure of the reservoir in psf

p_v vapor pressure in psf

p^* piezometric pressure in the Navier-Stokes equation in psf

r radius to any point in the pipe in ft

r' dimensionless radius parameter = r/a

t time in seconds

v local velocity in fps

w local velocity in fps

w' dimensionless velocity parameter = w/V_o

z axial co-ordinate in the pipe in ft

α_n zero roots of the Bessel function

δ thickness of the pipe wall in ft

λ dummy variable used in the solution of the Navier-Stokes equation

ν kinematic viscosity in ft^2/sec

ρ mass density in $lb\text{-}sec^2/ft^4$

τ_o boundary shear in psf

SUMMARY

An area of water-hammer research which has received relatively little attention is that of the generation of compression shock waves following the collapse of a vapor cavity. A laboratory investigation was performed in which the transient pressures upstream from a valve were examined. Theoretical analyses for the same system were also conducted. Two analyses were based on incompressible-flow theory, and a third was based on compressible-flow considerations.

Pressure-time records were obtained at a point immediately upstream from the valve by means of a pressure transducer and an oscillograph-recorder. Examination of these records indicated that cavitation had occurred and that the cavity existed for several times longer than the time for a compression wave to travel to the reservoir and return to the valve.

Theoretical results were superposed on the experimental records. The magnitudes of the incompressible-flow analyses varied considerably from the experimental results except for the initial compression wave in which correlation was very close. Close agreement of compressible-flow theory and experimental results was examined. It was concluded that when the time of vapor-cavity existence is less than ten times greater than the time for a compression shock wave to travel to the reservoir and return to the valve, compressible-flow analysis must be used.

CHAPTER I

INTRODUCTION

Definition of the Problem

Water-hammer, or the formation of shock waves resulting from the collapse of a vapor pocket, is little known. Despite fairly complete studies (both experimental and analytical) of water-hammer, this method of shock-wave generation has received relatively little attention.

Water-hammer is the name given to the pressure fluctuations which occur following the rapid deceleration of a column of liquid. Water-hammer can occur in many different places, as, for example, downstream from a valve. The inertia of the water causes separation to occur at the valve after closure. If the pressure is great enough at the extreme downstream end of the pipe, the liquid column will be decelerated toward the downstream end of the pipe, stopped, and then accelerated toward the valve. When the liquid strikes the valve, water-hammer pressures are produced.

Another cause of water-hammer, related to vapor-pocket formation, is that of cavitation in centrifugal pumps. If the pressure in the impeller is decreased, water-hammer occurs following the collapse of the vapor cavity. This flow condition has been observed in the pumping of phosphate slurry, for example. A partial plug caused by a stiff slug of slurry in the suction line followed by a sudden unplugging has resulted in extremely high pressures which occasionally caused pumps to

"blow up."

Probably the best-known example of water-hammer is that which occurs following the rapid closure of a downstream valve. This form of water-hammer is common in many residence plumbing systems. The loud banging which can be heard following valve closure is caused by shock waves moving in the pipe upstream from the valve.

According to classic water-hammer theory, upon closure of a downstream valve, a pressure wave or compression shock wave of magnitude ρVc moves upstream to the reservoir where it is reflected as a decompression shock wave and returns to the valve. The time of the round trip is $2L/c$, in which ρ is the density, V is the velocity prior to closure, c is the celerity of the shock wave, and L is the length of pipe. At the time the return wave reaches the valve, the pressure changes in the amount $2\rho Vc$ and another wave makes the round trip in $2L/c$ seconds.

In many instances, the pressure at the valve would be less than the vapor pressure of the liquid after the second shock wave emanates from the valve. In such cases, cavitation occurs at the valve. The vapor cavity exists for several times greater than $2L/c$ before it collapses. Upon collapse, another high-pressure shock wave is generated which makes the round trip to the reservoir and back to the valve in $2L/c$ seconds.

Fig. 1 shows the variation of pressure with time at the valve according to classic theory, neglecting dissipation. Fig. 2 shows the pressure-time variation at the valve when cavitation occurs.

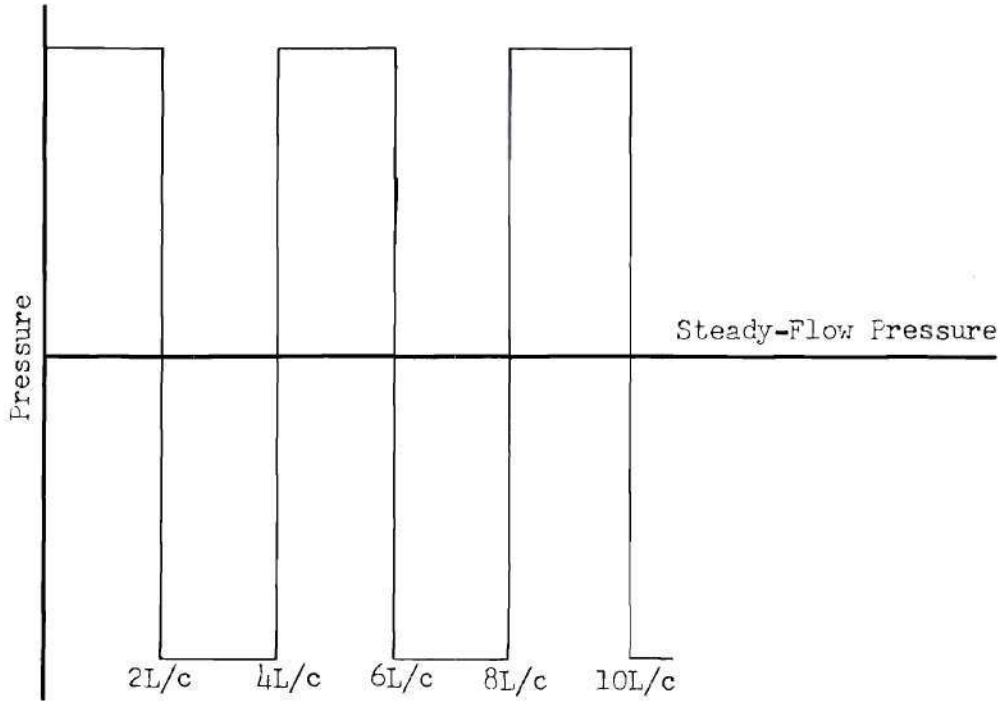

Figure 1. Pressure Variation According to Classic Theory

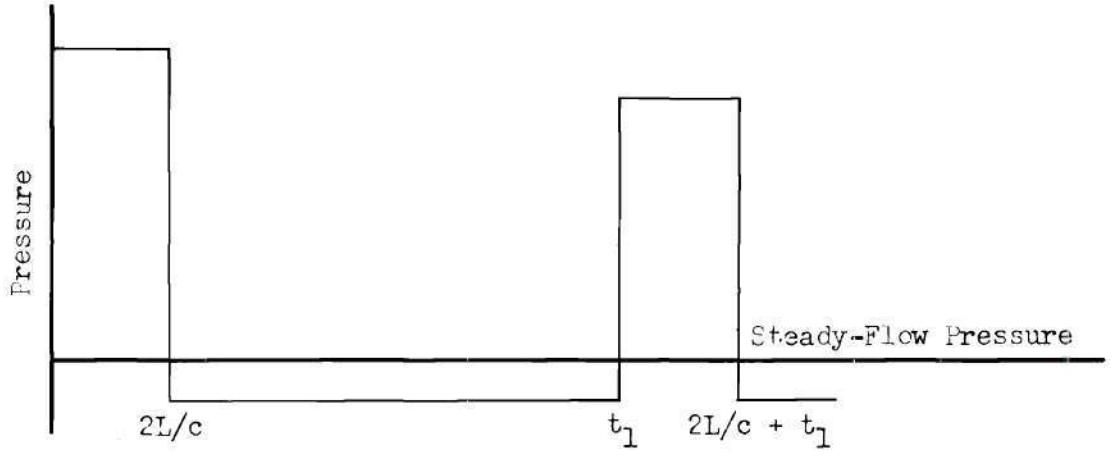

Figure 2. Pressure Variation after the Occurrence of Cavitation

Review of Literature

There have been very few investigations in the past which were concerned with vapor pocket formation upstream from a valve. Leconte (1) made experimental and theoretical analyses in 1937. He showed that a vapor pocket does form at the valve. Beginning with an equation of linear momentum, he derived equations which predict the time that the vapor cavity exists, and the magnitude of the following positive wave. Leconte uses a "coefficient of restitution" as a correction factor for his velocities. This coefficient changes for every pipe, and even between succeeding waves in a single pipe. Therefore, it is difficult to predict what the coefficient will be. For his own experimental apparatus, Leconte was able to predict his results with reasonable accuracy.

Bergeron (2) presented a graphic analysis of the problem of vapor cavity formation upstream from a valve. His presentation was based on the concept that shock waves are continually in motion in the liquid column between the upstream end of the vapor cavity and the reservoir. In other words, his analysis is based on compressible flow theory.

In the graphic analysis, friction is assumed to be concentrated at one or more points along the conduit. Bergeron presented a solution to the problem of vapor-cavity formation upstream from a valve in which pipe friction was assumed to be concentrated at the point where the conduit enters the reservoir. Since his analysis corresponds very closely to the physical circumstances of the present investigation, Bergeron's method is used as one means of analysis.

Objectives

The objectives of this investigation are twofold. First, it will be shown that cavitation does occur upstream from the valve after rapid closure. Second, two analyses based on purely dynamic (incompressible flow) considerations will be presented. A third analysis based on compressible flow will also be given. It will be shown that for the experimental system in this investigation the compressible-flow results correspond much more closely to the experimental results than do the results of the incompressible flow analyses.

CHAPTER II

THEORETICAL ANALYSIS

General

The problem under consideration is an investigation of the phenomena occurring in a pipeline after the instantaneous closure of a downstream valve. In particular, the flow characteristics just upstream from the valve are presented.

Upon closure of the valve a compression shock wave is generated at the valve which travels toward the reservoir with the celerity c. The fluid column is at rest behind the wave; that is, between the wave front and the valve. During this period the well-known classical water-hammer theory is presumed to be applicable. Equations resulting from this theory are summarized in the following. For celerity

$$c = \sqrt{\frac{E_w/\rho}{1 + \frac{E_w D}{E_p \delta}}} \qquad (1)$$

in which c is the wave celerity in ft/sec, E_w is the bulk modulus of elasticity of the liquid in psf, E_p is the modulus of elasticity of the pipe-wall material, in psf, D is the inside diameter of the pipe in feet, δ is the wall thickness in feet, and ρ is the liquid density in lb-sec^2/ft^4. For pressure at the valve

$$p = p_a + \rho c V_o \qquad (2)$$

in which p is the pressure at the valve in psf, and p_a is the piezometric pressure at the valve immediately before the compression shock wave is generated in psf.

During the time interval from L/c to $2L/c$ a decompression wave moves from the reservoir toward the valve. The compressed liquid, which is at rest, is decompressed through the wave and the liquid is again in motion but in the opposite direction to the initial flow.

At the time $2L/c$ the wave of decompression reaches the valve. The liquid is now all in motion toward the reservoir. According to classic theory another decompression wave would be generated at the valve at this time which would move toward the reservoir leaving behind a fluid at rest and at greatly reduced pressures. However, in many situations the pressure behind this wave is less than the vapor pressure of the liquid. In such a case, the liquid will change to the gas state with the formation of a vapor cavity adjacent to the valve.

The following analyses apply for the time during which a vapor cavity exists near the valve. Inasmuch as the duration of the vapor cavity is several times greater than $2L/c$, the first analysis of the growth and decay is based on the dynamic equations of incompressible flow. (Using the assumption of incompressible flow two separate results are presented.) In the first presentation the assumption is that during the existence of the vapor cavity, the flow in the liquid column is turbulent. In the second presentation the assumption is that the flow is laminar.

The second analysis is based upon work done by Bergeron (2). In this analysis, it is assumed that even though separation has occurred at the valve, elastic waves still travel from the cavity to the reservoir and back. In addition, resistance forces are assumed to be the same as for steady flow and to be concentrated at the reservoir end of the pipe. In other words, compressible-flow theory is applied to the liquid column in the pipe.

The results of both analyses, as well as experimental results, are presented in the following sections. Several conclusions are drawn from the comparison of results.

Incompressible-Flow Analyses

Turbulent Flow

It is assumed in this analysis that during the growth and decay of the vapor cavity the flow is turbulent and that friction varies according to Blasius' Law, $f = \frac{0.3164}{R^{1/4}}$ in which R is the Reynolds Number. It is also assumed that the length of the vapor cavity is negligible in relation to the total length of the pipe, L. In Fig. 3 are shown sketches of the prevailing conditions as the cavity grows and decays.

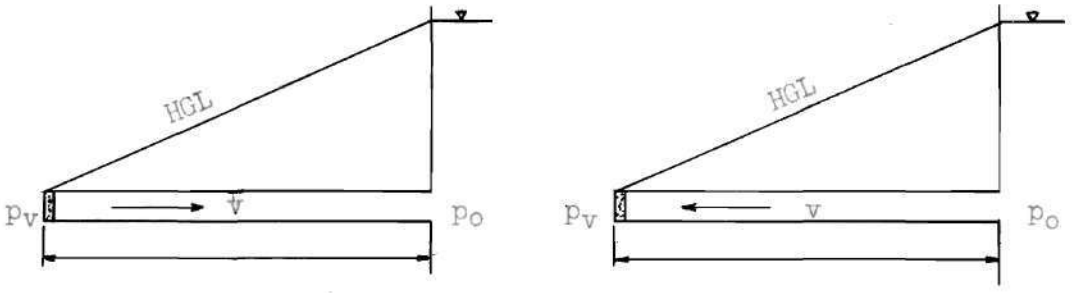

a. Growth b. Decay

Figure 3. Conditions During the Vapor Cavity Existence

The linear momentum equation for the above system, including friction, is

$$p_v A - p_o A - \tau_o CL = \rho L A \frac{dV}{dt} \tag{3}$$

in which p_v is the vapor pressure in psia, p_o is the static pressure at the reservoir in psia, A is the area of the pipe in ft^2, τ_o is the boundary shear in psf, C is the perimeter of the pipe in ft, and L is the length of the pipe in ft. Assuming that Blasius' expression for steady flow in a pipe is applicable to unsteady flow,

$$\tau_o = \frac{0.3164\ \nu^{1/4}}{V^{1/4}\ D^{1/4}} \frac{\rho V^2}{8} \tag{4}$$

Combining Equation (3) and Equation (4)

$$(p_v - p_o)A - \frac{0.3164\ \nu^{1/4}\ \rho V^{\frac{7}{4}} CL}{2\ D^{5/4}} = \rho L A \frac{dV}{dt}$$

Resulting in

$$\frac{-(p_o - p_v)}{\rho L} - \frac{0.3164\ \nu^{1/4}\ V^{7/4}}{2\ D^{5/4}} = \frac{dV}{dt} \tag{5}$$

Equation (5) can be made dimensionless by introducing the following parameters:

$$t' = \frac{\nu t}{a^2}$$

$$P' = \frac{-(p_o - p_v)a^2}{\rho L V_o \nu}$$

$$V' = V/V_o$$

Equation (5) then becomes

$$P' - \frac{0.3164}{8} \frac{D^{3/4} \nu^{3/4}}{\nu^{3/4}} (V')^{7/4} = \frac{dV'}{dt'}$$

or

$$P' - 0.03955\, R^{3/4} (V')^{7/4} = \frac{dV'}{dt} \qquad (6)$$

$$dV' = (P' - 0.03955\, R^{3/4} V'^{7/4})\, dt \qquad (7)$$

Equation (7) cannot be easily integrated. Therefore, the following approximate form was programmed for numerical solution on the Burroughs 220 Electronic Computer at the Rich Electronic Computer Center at Georgia Tech:

$$\Delta V = (P' - 0.03955\, R^{3/4} V'^{7/4})\, \Delta t \qquad (8)$$

For each increment of time a new value of V' was taken where $V'_n = V'_{n-1} + \Delta V$ in a manner similar to that used by McNown (3).

Laminar Flow

In this analysis the assumptions are that the pipe is straight, that the flow is laminar, that the initial velocity distribution is uniform, and that the length of the vapor cavity is negligible.

At the instant the vapor cavity begins to form, the water in the pipe is all moving toward the reservoir. The velocity is equal to the velocity with which the water struck the valve and the flow conditions are the same as those shown in Fig. 3a.

The Navier-Stokes equation along the axial co-ordinate is

$$-\frac{1}{\rho}\frac{\partial p^*}{\partial z} = \frac{\partial v}{\partial t} - \nu\left(\frac{\partial^2 v}{\partial r^2} + \frac{1}{r}\frac{\partial v}{\partial r}\right) \qquad (9)$$

The axial direction, z is taken as positive in the direction toward the reservoir. The following conditions prevail throughout the system:

$$P = -\frac{1}{\rho}\frac{\partial p^*}{\partial z} = \frac{-(p_o - p_v)}{\rho L}$$

$$V = f(r\ ,\ t)$$

The initial condition at $t = 0$ is

$$v(r\ ,\ 0) = +U_o$$

The boundary condition for $t > 0$ is

$$v(a\ ,\ t) = 0$$

in which a is the radius of the pipe in ft.

The Navier-Stokes Equation (9) can be transformed into a form for which the solution has been previously found. Letting

$$v = w + V_o + Pt$$

the Navier-Stokes equation then becomes

$$\frac{\partial w}{\partial t} = \nu \left(\frac{\partial^2 w}{\partial r^2} + \frac{1}{r} \frac{\partial w}{\partial r}\right) \tag{10}$$

Changing to dimensionless variables for ease of solution as follows,

$$w' = \frac{w}{V_o}$$

$$r' = \frac{r}{a}$$

$$t' = \frac{\nu t}{a^2}$$

$$P' = \frac{Pa^2}{V_o \nu}$$

Differentiating the dimensionless parameters and substituting into Equation (10)

$$\frac{V_o \nu}{a^2} \frac{\partial w'}{\partial t'} = \frac{V_o \nu}{a^2} \left(\frac{\partial^2 w'}{\partial r'^2}\right) + \frac{V_o \nu}{a^2} \frac{1}{r'} \frac{\partial w'}{\partial r'}$$

or

$$\frac{\partial w'}{\partial t'} = \frac{\partial^2 w'}{\partial r'^2} + \frac{1}{r'} \frac{\partial w'}{\partial r'} \tag{11}$$

Substituting

$$w = v - V_o - Pt$$

w' is expressible in terms of the other dimensionless variables

$$w' = \frac{V}{V_o} - 1 - \frac{Pt}{V_o} = \frac{V}{V_o} - 1 - \frac{a^2 P}{\nu V_o}\left(\frac{\nu t}{a^2}\right) = v' - 1 - P't'$$

The initial condition is

$$w'(r' , 0) = 0$$

The boundary condition is $w'(1 , t') = -(1 + P't')$.

The solution of the partial differential equation, Equation (9), is given by Carslaw and Jaeger (4).

$$w' = 2 \sum_{n=1}^{\infty} e^{-\alpha_n^2 t'} \alpha_n \frac{J_o(r' \alpha_n)}{J_1(\alpha_n)} \int_o^{t'} e^{\alpha_n^2 \lambda} (- 1 - P' \lambda) d\lambda \quad (12)$$

in which J_o is the Bessel coefficient of order zero, J_1 is the Bessel coefficient of order one, α_n are the zero roots of the Bessel function, and λ is a dummy variable.

Evaluating the integral:

$$I_1 = - \int_o^{t'} e^{\alpha_n^2 \lambda} d\lambda = \left(- \frac{1}{\alpha_n^2} e^{\alpha_n^2 \lambda}\right) \Bigg|_o^{t'} = \frac{1}{\alpha_n^2}\left(1 - e^{\alpha_n^2 t'}\right)$$

$$I_2 = - P' \int_o^{t'} e^{\alpha_n^2 \lambda} \lambda \, d\lambda = P' \left[\frac{e^{\alpha_n^2 \lambda}}{\alpha_n^4} \left(\alpha_n^2 \lambda - 1\right) \right]_o^{t'}$$

$$= \frac{P'}{\alpha_n^4}\left[e^{\alpha_n^2 t'}(\alpha_n^2 t' - 1) - (-1) \right] = \frac{-P'}{\alpha_n^4}(1 - e^{\alpha_n^2 t'}) - \frac{P't'e^{\alpha_n^2 t'}}{\alpha_n^2}$$

$$I_1 + I_2 = \frac{1}{\alpha_n^2}(1 - \frac{P'}{\alpha_n^2})(1 - e^{\alpha_n^2 t}) - \frac{P't'e^{\alpha_n^2 t'}}{\alpha_n^2}$$

with the result that

$$w' = 2\sum_{n=1}^{\infty} e^{\alpha_n^2 t'} \alpha_n \frac{J_o(r'\alpha_n)}{J_1(\alpha_n)}(\frac{1}{\alpha_n^2})\left[(1 - \frac{P'}{\alpha_n^2})(1 - e^{\alpha_n^2 t'}) - P't'e^{\alpha_n^2 t'} \right]$$

$$= 2\sum_{n=1}^{\infty} \frac{J_o(r'\alpha_n)}{\alpha_n J_1(\alpha_n)}\left[(\frac{P'}{\alpha_n^2} - 1)(1 - e^{\alpha_n^2 t'}) - P't' \right] \qquad (13)$$

Solving for the mean velocity

$$V = \frac{1}{a^2\pi}\int_o^a v\, 2\pi\, r\, dr = \frac{2\pi}{a^2\pi} V_o a^2 \int_o^1 \frac{v}{V_o} r'\, dr'$$

$$\frac{V}{V_o} = 2\int_o^1 (\frac{v}{V_o})\, r'\, dr' = 2\int_o^1 (\frac{w}{V_o} + 1 + P't')\, r'\, dr'$$

$$= 2\int_o^1 w'\, r'\, dr' + 1 + P't' \qquad (14)$$

By substituting Equation (13) into Equation (14) and integrating, the mean velocity at any time can be found. Since the expression $J_o(r'\alpha_n)$

is the only term containing r', this expression can be evaluated in the integral.

$$\int_0^1 J_o(r' \alpha_n) r' \, dr' = \frac{J_1(\alpha_n)}{\alpha_n}$$

Combining Equation (13), Equation (14), and Equation (15) in order to obtain an expression for the mean velocity

$$\frac{V}{V_o} = 1 + P't' + 4 \sum_{n=1}^{\infty} \frac{1}{\alpha_n^2} \left[\left(\frac{P'}{\alpha_n^2} - 1 \right)\left(1 - e^{-\alpha_n^2 t'}\right) - P't' \right] \qquad (16)$$

Since values of α_n increase rapidly it was assumed that the first ten values of α_n would approximate the summation closely enough for practical results. The following modified form of Equation (16) was programmed for solution on the Burroughs 220 Computer.

$$\frac{V}{V_o} = 1 + P't' + 4 \sum_{n=1}^{10} \frac{1}{\alpha_n^2} \left[\left(\frac{P'}{\alpha_n^2} - 1 \right)\left(1 - e^{-\alpha_n^2 t'}\right) - P't' \right] \qquad (17)$$

Effect of Pressure Gradient

As a wave travels toward the reservoir, it encounters increased resistance because of the increase in pressure due to the pressure gradient. A derivation of the equations for pressure increase is given by McNown (3) and thus, only the final result will be given here. The maximum pressure increase at the valve due to the pressure gradient is $\Delta p/\sqrt{2}$ in which Δp is the pressure drop from the reservoir to the valve.

Compressible Flow Analysis

For a complete discussion of graphic methods of water-hammer analysis, the reader is referred to Bergeron (2). The method for solution of vapor cavity formation upstream from a valve is outlined below. First, the framework of the diagram is drawn, as shown in Fig. 4. Ordinates on the framework denote pressure, abscissas depict discharge. The framework includes the vertical axis representing pressure, the bottom solid line representing vapor pressure, and the parabolic curve representing pressure versus discharge at the valve. To the right of the vertical axis, the parabola depicts conditions for water flowing from the reservoir toward the valve. Conditions for the water flowing from the valve toward the reservoir are shown to the left of the axis. This curve was determined experimentally by steady-flow tests.

Next, the overpressure ($p = \rho cV$) is plotted on the vertical axis. It should be recalled that for the first wave, this overpressure rises from steady-flow pressure rather than from vapor pressure. Since $p = \rho cV = \frac{cQ}{A}$ or $\frac{p}{Q} = \frac{c}{A}$ = constant , straight lines connect points on the diagram and represent the passage of a wave from location in the pipe to another location. The line $\overline{0_A 2_A}$ in Fig. 5 denotes the instantaneous pressure rise at the valve immediately after valve closure.

The fluid at the valve remains at the high overpressure (point 2_A) until the compressive wave returns to the valve. At this time, the pressure drops immediately to vapor pressure (point 4_A). Elastic waves of low pressure (line $\overline{4_A 5_B}$, etc.) travel between the valve and the reservoir until the vapor cavity collapses.

Figures 6 and 7 show the analysis for Run 3, which was a typical run. The procedure used was identical for all runs.

To determine the time of collapse, a plot of discharge versus time is made (Fig. 7). When the area under the negative discharge curve equals the area under the positive discharge curve, the cavity collapses. Discharges for this plot are scaled from the pressure-discharge diagram (Fig. 6).

It usually happens that the cavity collapses while a low-pressure wave is traveling in the conduit. There is an initial pressure rise due to the collapse of the cavity. When the elastic wave reaches the valve, there is an additional pressure rise. This rise can be seen in the stepped construction of the second wave in Fig. 7.

The process can be continued through as many cycles as are necessary. For more than two cycles, it is expedient to draw supplementary pressure-discharge diagrams since the original diagram soon becomes cluttered.

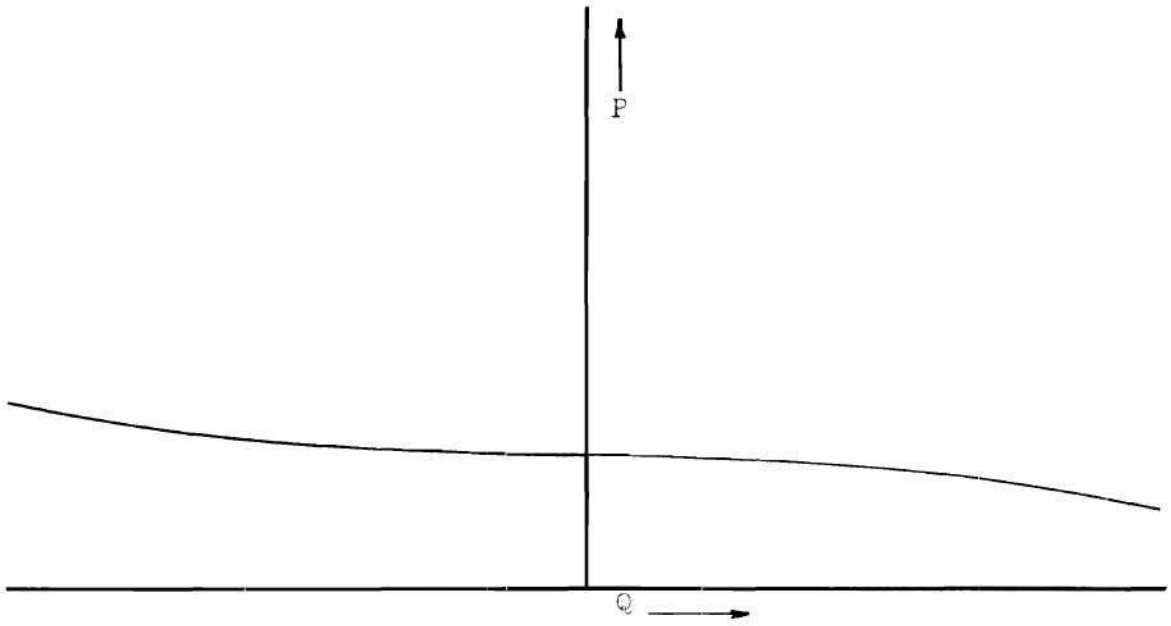

Figure 4. Initial Framework

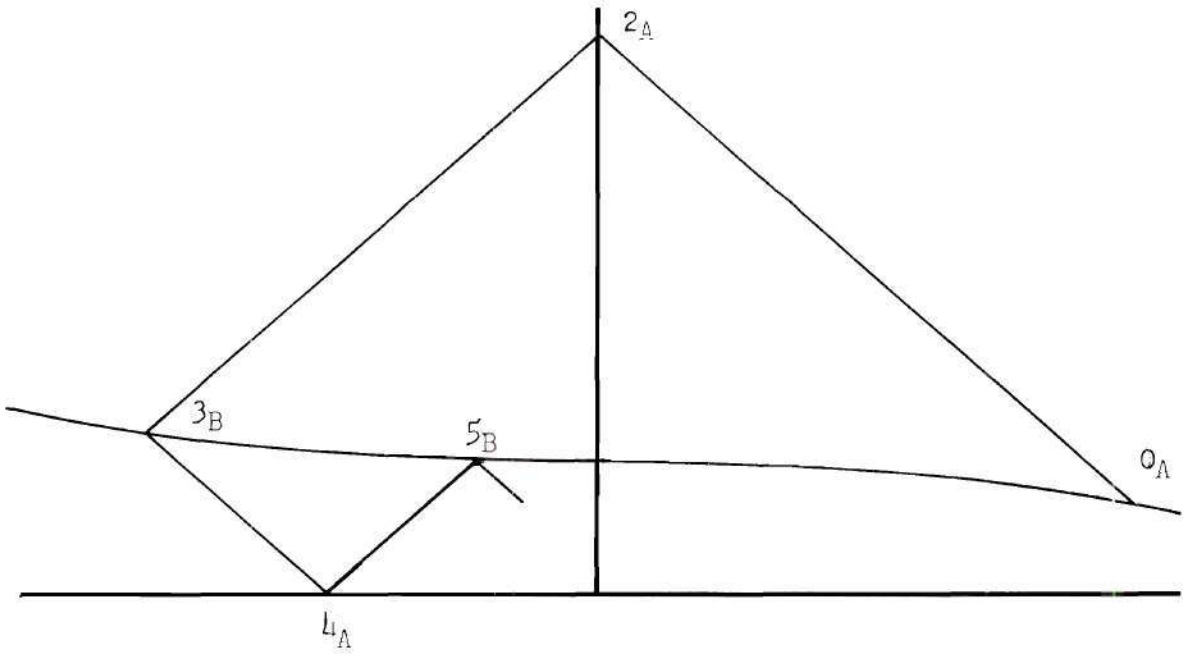

Figure 5. First Pressure Wave

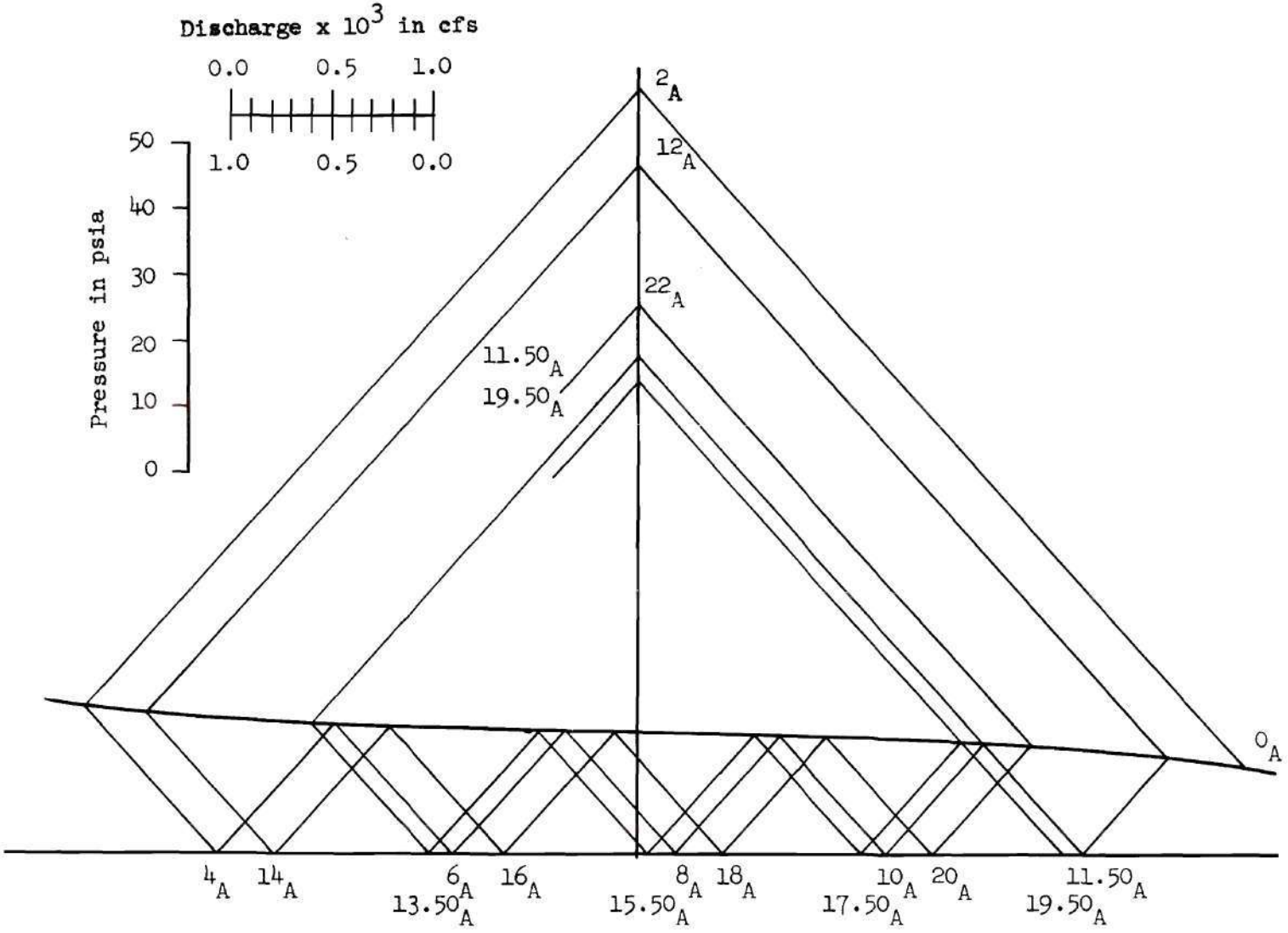

Figure 6. Elastic-Wave Diagram

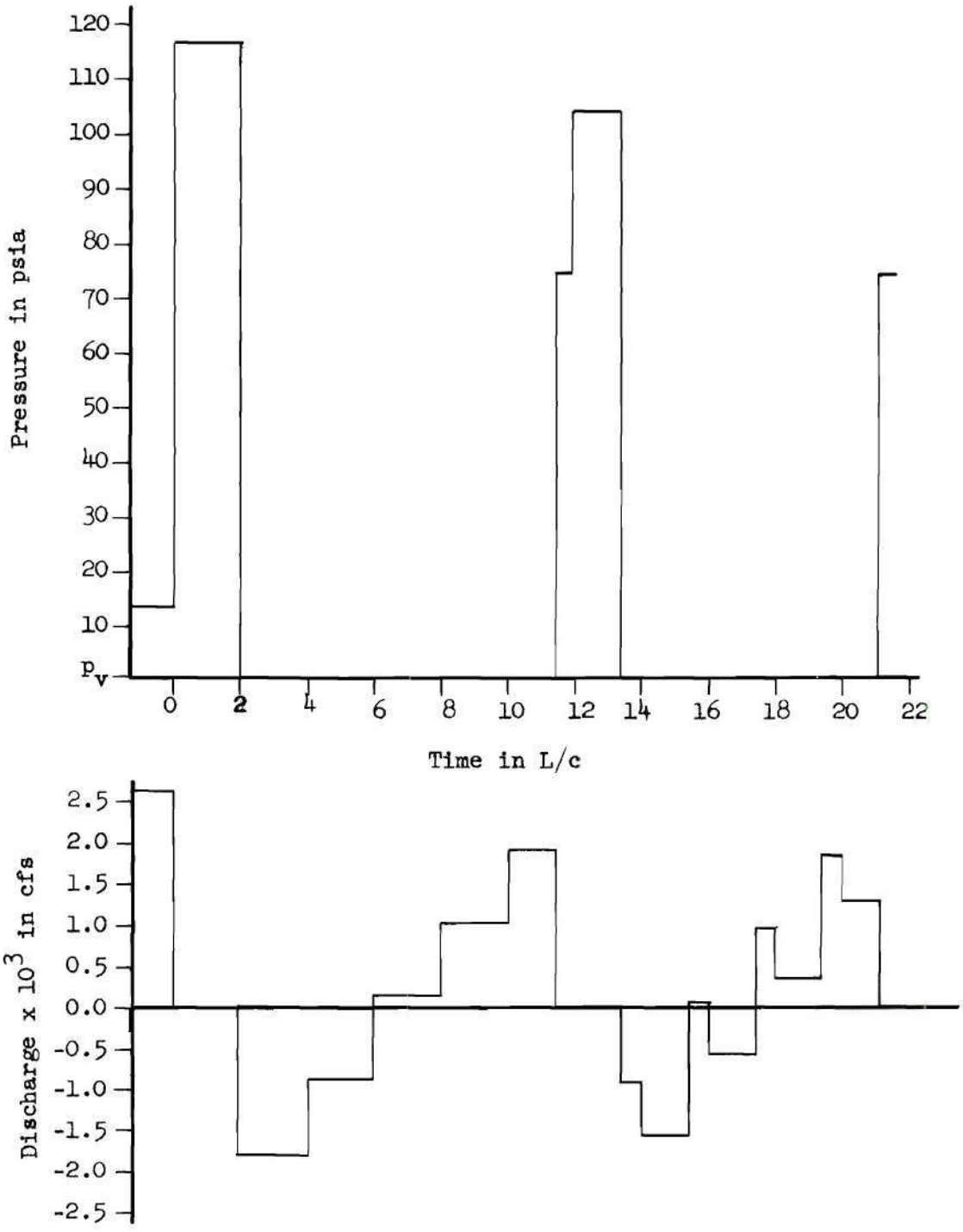

Figure 7. Time Variations of Pressure and Discharge

CHAPTER III

INSTRUMENTATION AND EQUIPMENT

General

An apparatus for generating and measuring water-hammer pressures was constructed and installed in the Hydraulics Laboratory of the School of Civil Engineering in order to study experimentally the phenomenon of vapor cavity formation and decay. The installation is permanent in order that the apparatus can be used for demonstration and teaching purposes in graduate and undergraduate hydraulics courses.

Tubing and Valves

The apparatus consisted of a single length of 5/8-inch O.D. copper tubing 334 feet long. The tubing was rolled into 33 coils, with each coil being 36 inches in diameter and lying directly on the preceeding coil. A rigid steel frame was welded to contain the coils and to hold them in place. The entire device was then suspended from a concrete ceiling beam in the hydraulics laboratory. There was very little movement in the system, even with high-pressure waves traveling in the tubing.

The upstream end of the tubing was connected to a six-inch water line which was supplied by a constant-head tank. Since the water line was so much larger than the copper tubing, high-pressure waves in the tubing were reflected as from an infinite reservoir.

On the downstream end of the tubing, two valves were installed. The downstream valve was a slow-acting gate valve which was used for throttling the flow. The upstream valve was a quick-acting, hand-operated valve which could be slammed shut to produce the water-hammer waves.

Downstream from the throttling valve, a flexible line was attached to the tubing. This flexible line was connected to a weighing tank for measuring discharge.

Immediately upstream from the quick-operating valve and as close as possible to the valve was a "tee" to which the pressure transducer was connected. The proximity to the valve was desirable so that the frequency of waves traveling between the valve and the transducer would be greater than the frequency response of the transducer. These waves would have greatly complicated the data had they been recorded. Figure 8 shows the valves, and the transducer connected at the "tee".

Pressure Transducer and Recorder

A pressure transducer is a pressure-sensitive device which converts pressure changes into electrical-resistance changes. The transducer used was an unbonded strain-gage type, manufactured by Consolidated Instruments Corporation. The pressure range was 0-100 psi absolute with 250 per cent overload protection.

The resistance change from the transducer is received and amplified by a strain-gage amplifier. The amplifier is connected to an oscillograph which records the pressure changes. Before the recorded results can be interpreted, it is necessary that the transducer-recorder

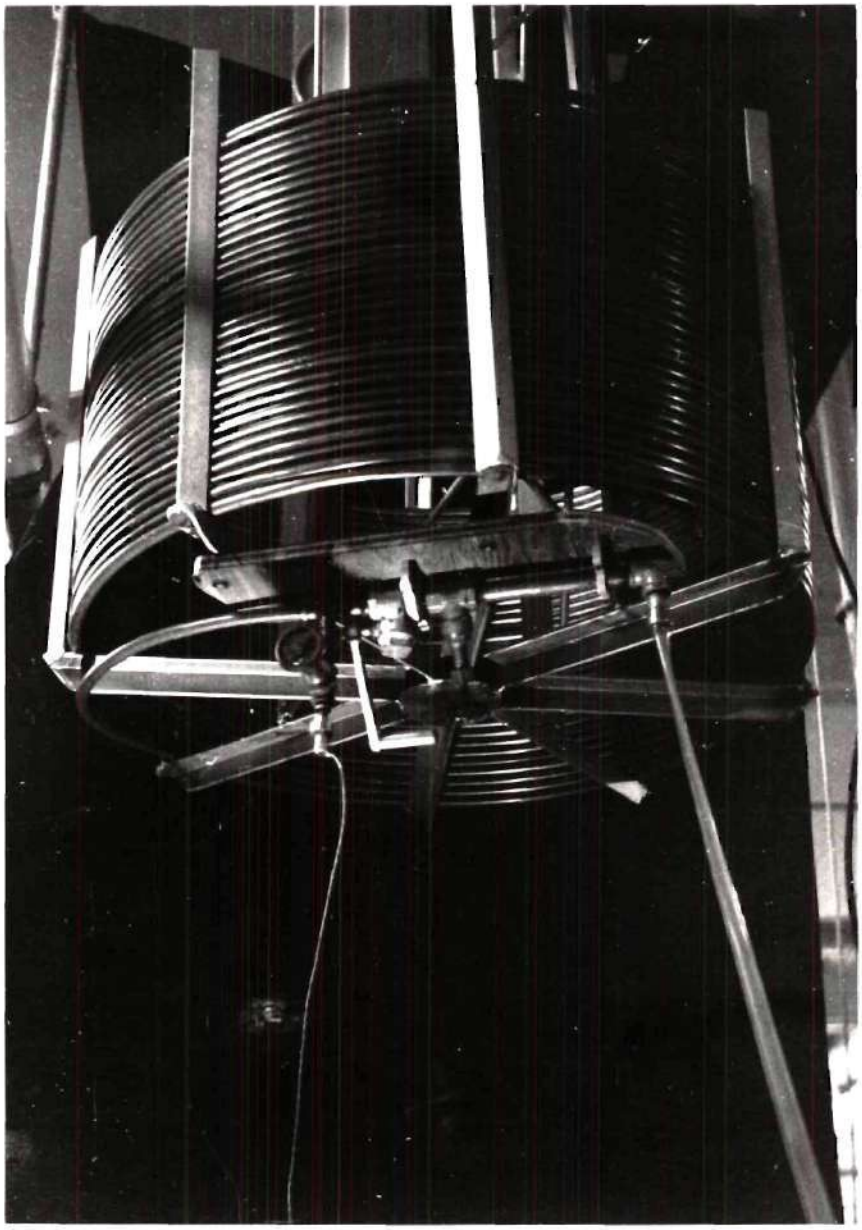

Figure 8. View Showing Tubing, Valves, and Transducer.

system be calibrated. Calibration procedure is described in Chapter IV, "Experimental Procedure." A Sanborn oscillograph recorder was used in the unsteady flow tests to measure the transient pressures from the transducer. The recorder is shown in Fig. 9.

Steady-Flow Instrumentation

For measuring steady-flow pressures at the valve, the transducer was replaced by a constant-displacement mercury manometer. During these tests, the quick-closing valve remained open at all times.

Figure 9. View of Recorder.

CHAPTER IV

EXPERIMENTAL PROCEDURE

Transient Pressure Measurement

A series of five runs was made in which the water-hammer pressures were measured. For each run, the discharge was varied by means of the throttling valve.

Before making the runs, and after completion of the runs, it was necessary to calibrate the transducer. The two calibrations were needed because the amplifier-recorder tended to shift slightly over a period of time. An Ashcroft dead-weight gage tester was used for calibration.

The transducer was calibrated by attaching it to the gage tester and connecting the recorder. It was found, as expected, that a straight-line relationship existed between the pressure and the recorder deflection. The slopes of the lines were computed by the method of least squares. Calibration curves are shown in Fig. 10.

Identical procedure was used for all runs in which transient pressures were measured. First, the discharge was measured gravimetrically. The recorder was then started and the quick-operating valve was slammed shut. After several cycles of waves had occurred, the recorder was stopped. During the time that the waves were traveling in the tubing, it could be detected by ear that the intensity of each compression wave was less than that of the preceding wave and that the time between decompression waves became smaller.

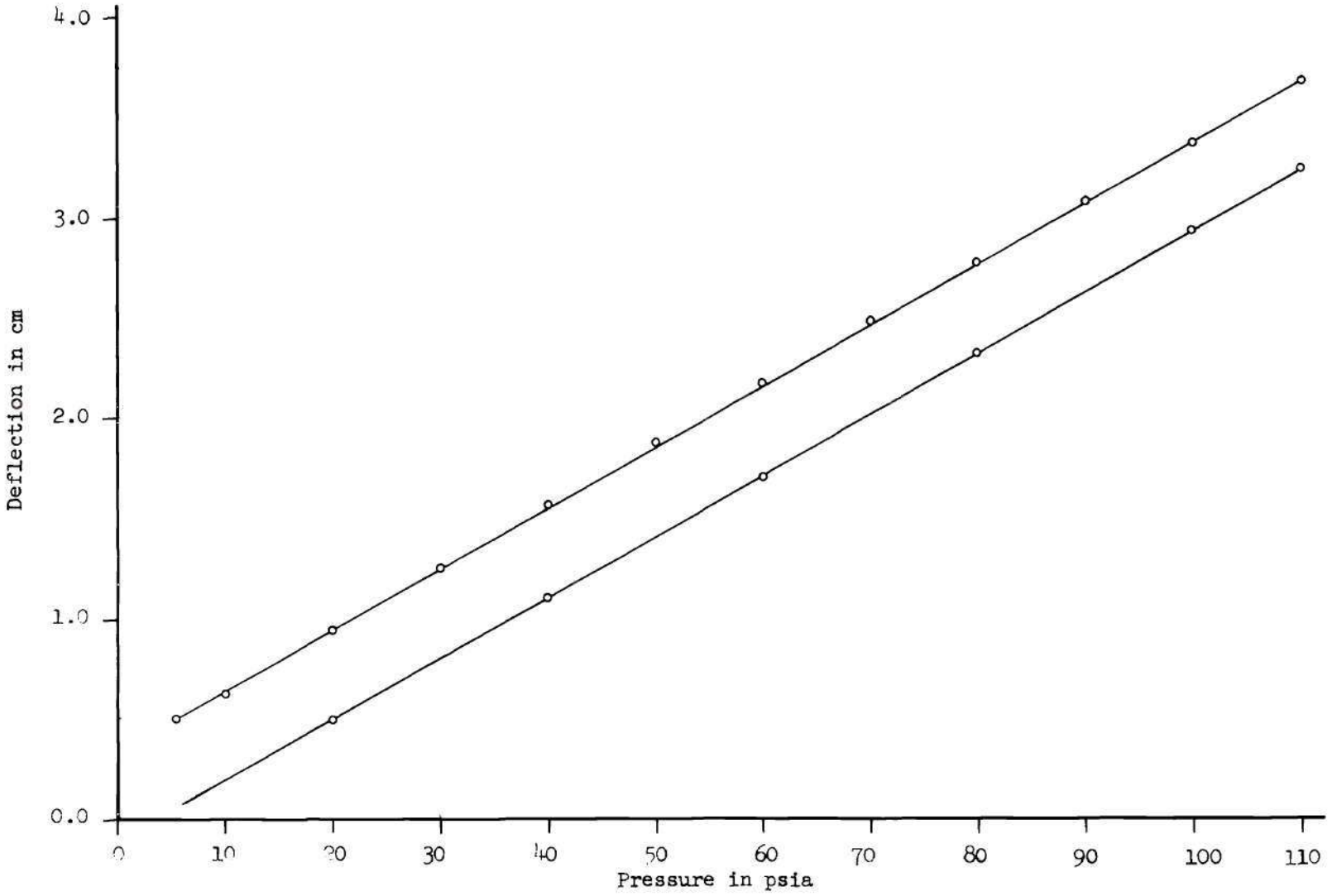

Figure 10. Transducer Calibration Curves

Steady-Flow Measurement

One series of runs was made using a differential mercury manometer as a pressure measuring device. The quick-operating valve remained open throughout these tests. The discharge was varied for each run by means of the throttling valve.

The purpose of this series of runs was to establish a curve (Fig. 11) of steady-flow pressure versus discharge. This curve was used to determine the initial pressures in the unsteady flow runs before the valve was slammed shut. The static pressure of the system with all valves closed was also measured at this time.

During both steady-flow runs and unsteady flow runs, the barometer was read. All pressures were then converted to absolute pressures.

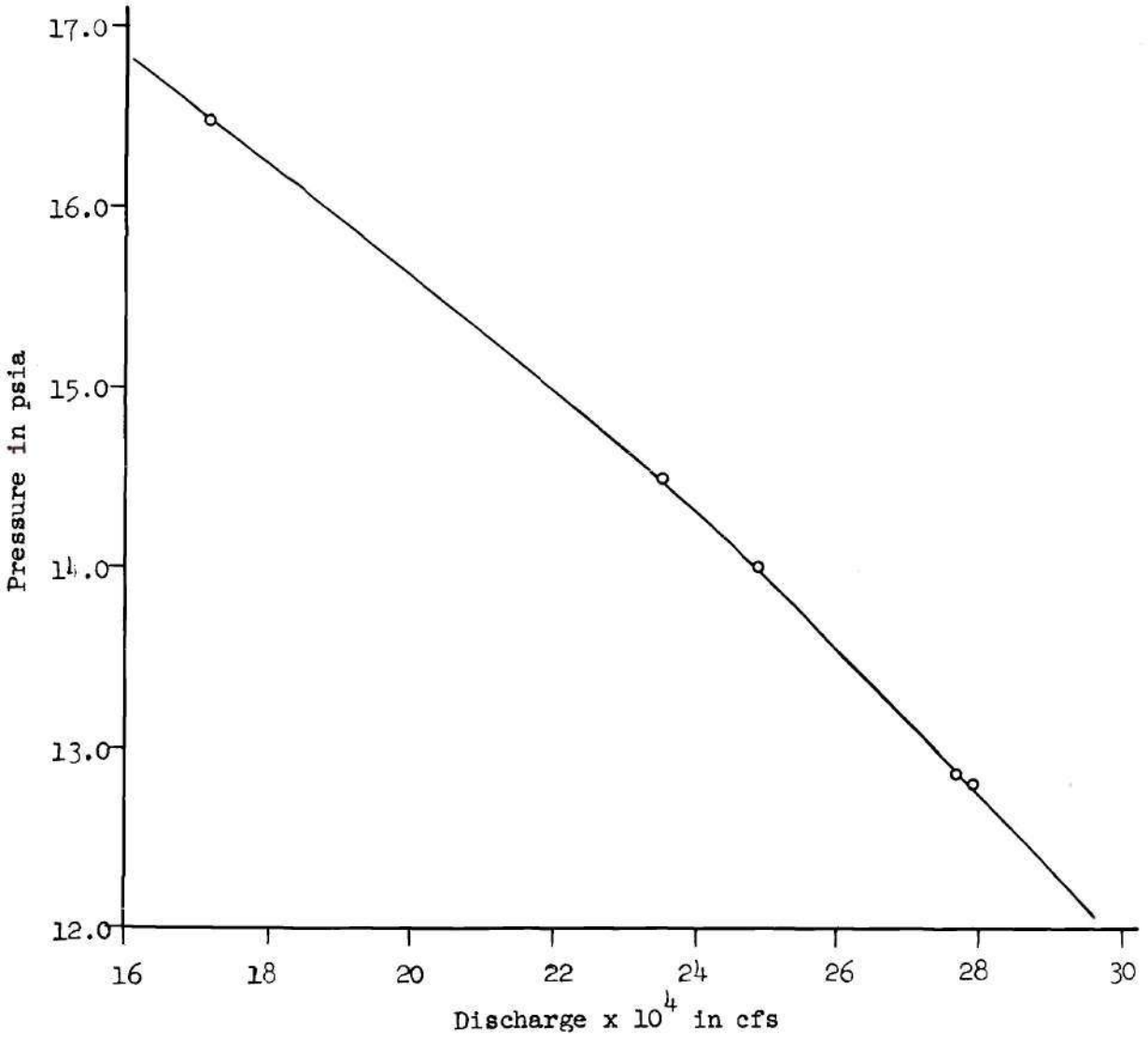

Figure 11. Steady-Flow Pressure at the Valve

CHAPTER V

DETERMINATION OF AND DISCUSSION OF RESULTS

Methods of Analysis

Equations (8) and (17) were solved numerically on the Burroughs 220 Computer. The computer values were interpolated to find the dimensionless time of collapse of the vapor cavity and the dimensionless velocity of collapse. Curves of these values were then plotted.

For each run, beginning with the initial velocity, P' and R were computed. Entering the velocity-of-collapse curve with the computed values of P' and R, a new velocity was read. This new velocity was used to compute the magnitude of the next positive wave and also to compute new values of P' and R. The times of existence of the vapor cavity were read from the appropriate curve using the initial and computed values of P' and R.

The numerical solutions for Equations (8) and (17) and the curves drawn from the solutions are on file in the Hydraulics Laboratory.

The graphic analysis by which the compressible-flow solutions were obtained is described in detail in Bergeron (2). A typical graphic solution is shown in Fig. 6 and 7. The results of the graphic analyses are shown in Fig. 12 through 16.

Analysis of Results

The experimental results which are shown in Fig. 12 through 16

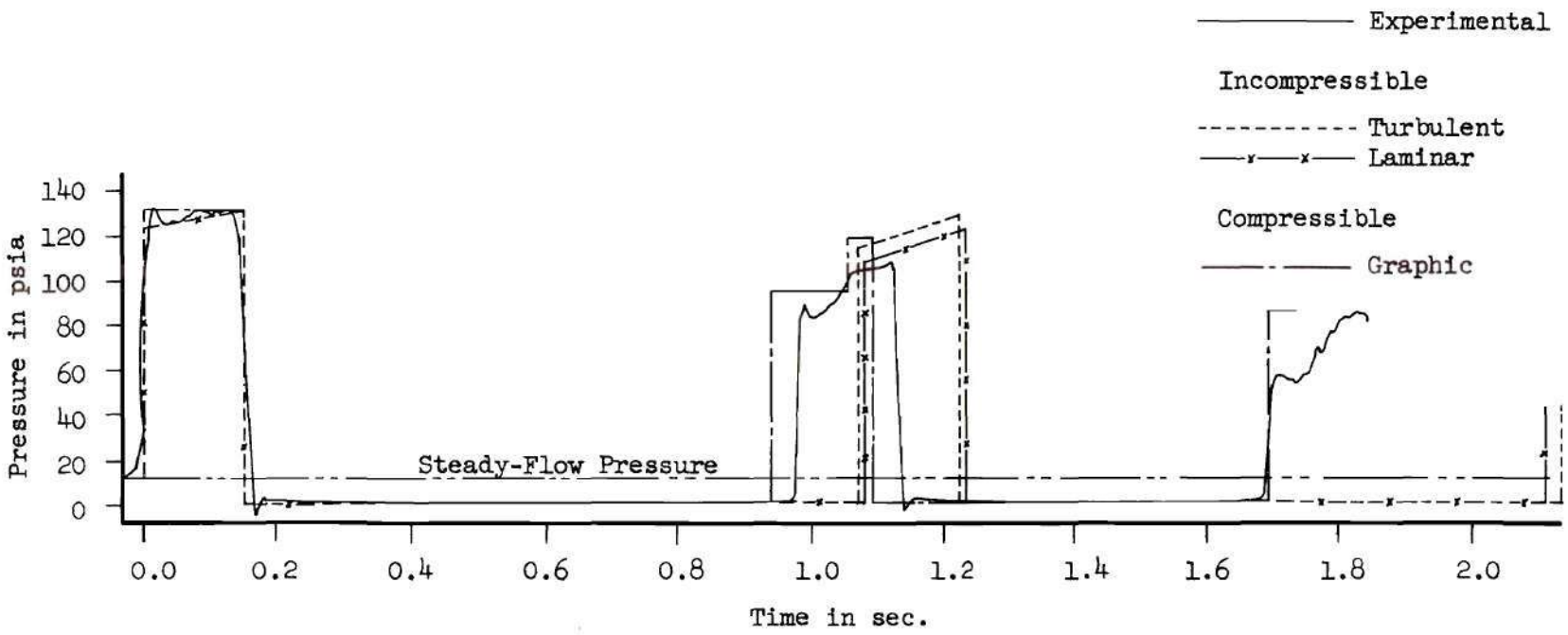

Figure 12. Experimental and Theoretical Results: Run 1

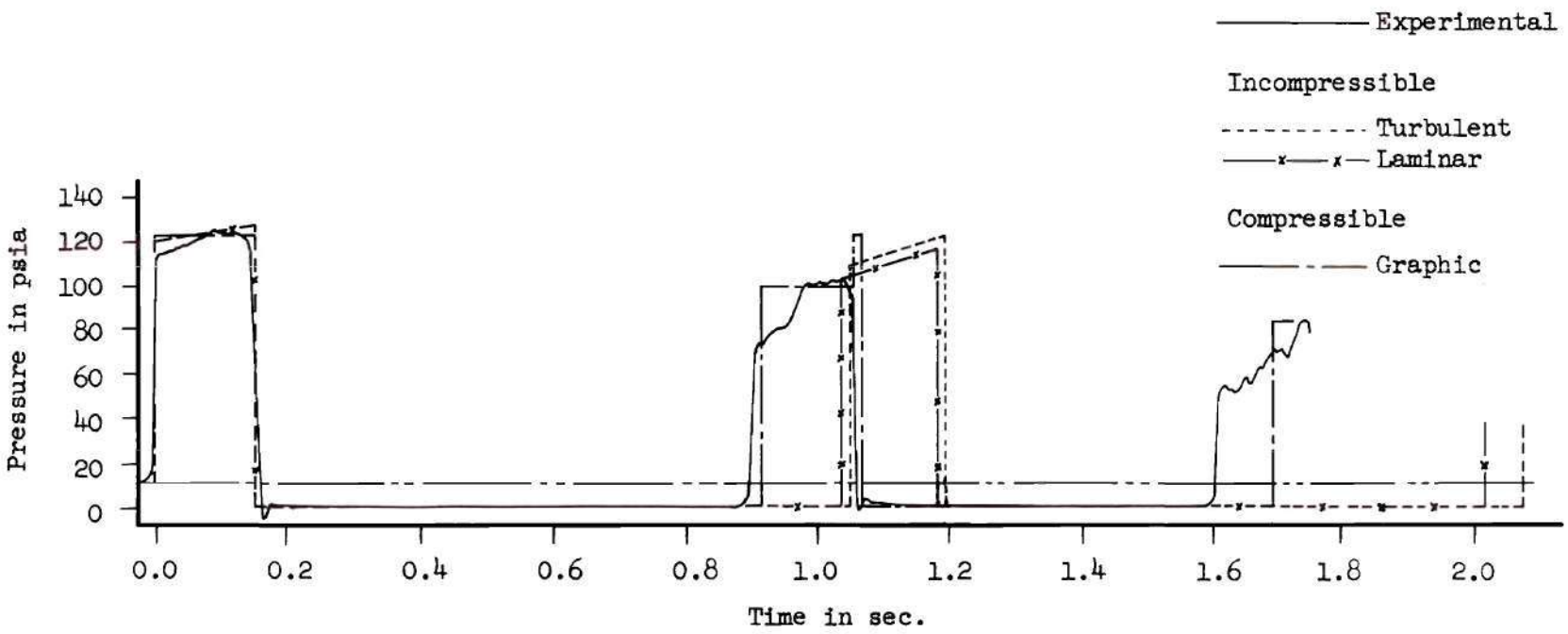

Figure 13. Experimental and Theoretical Results: Run 2

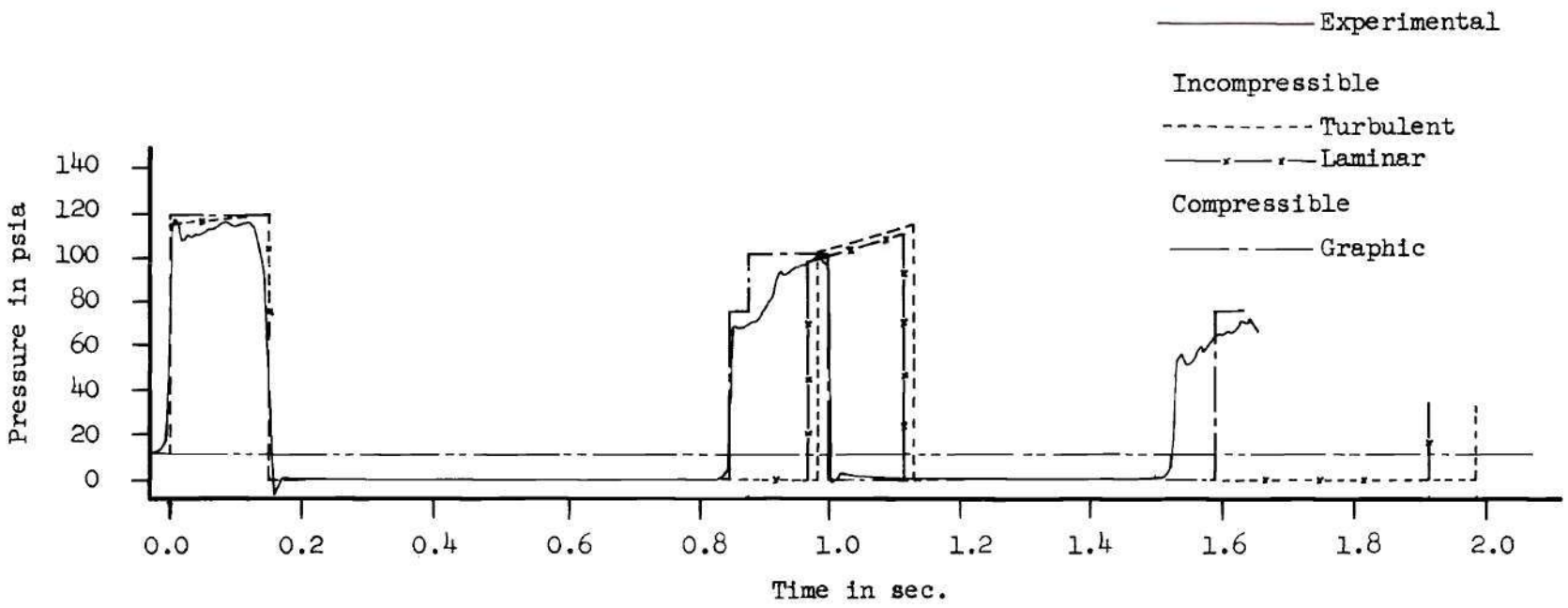

Figure 14. Experimental and Theoretical Results: Run 3

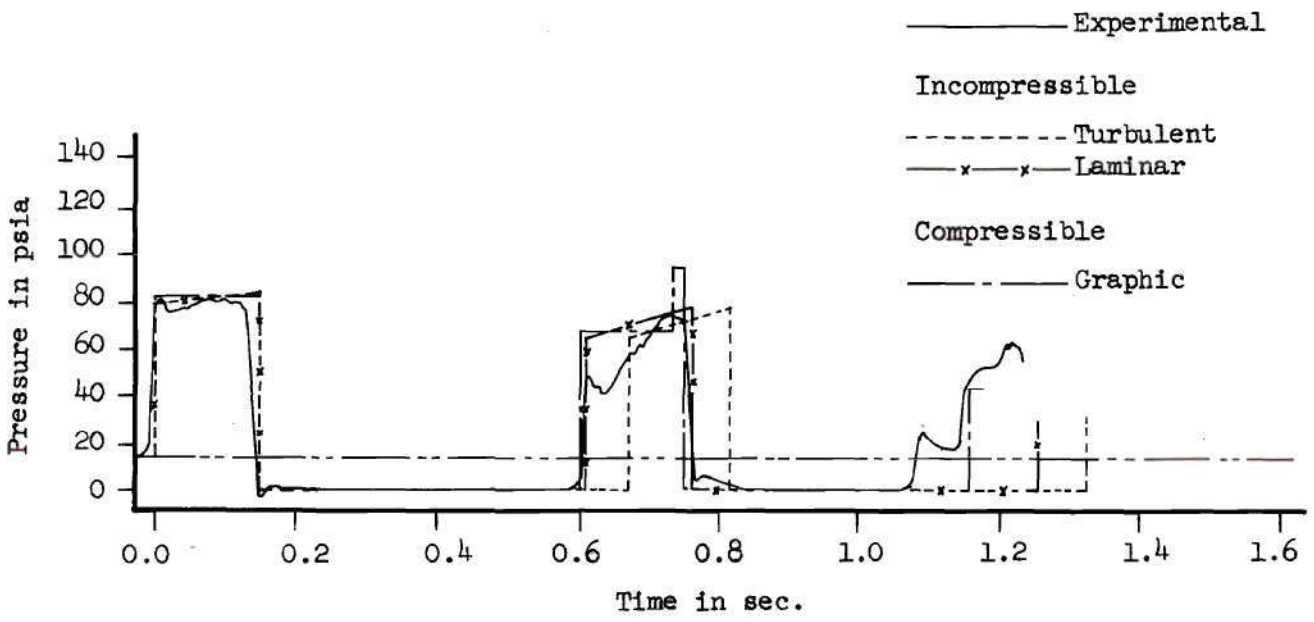

Figure 15. Experimental and Theoretical Results: Run 4

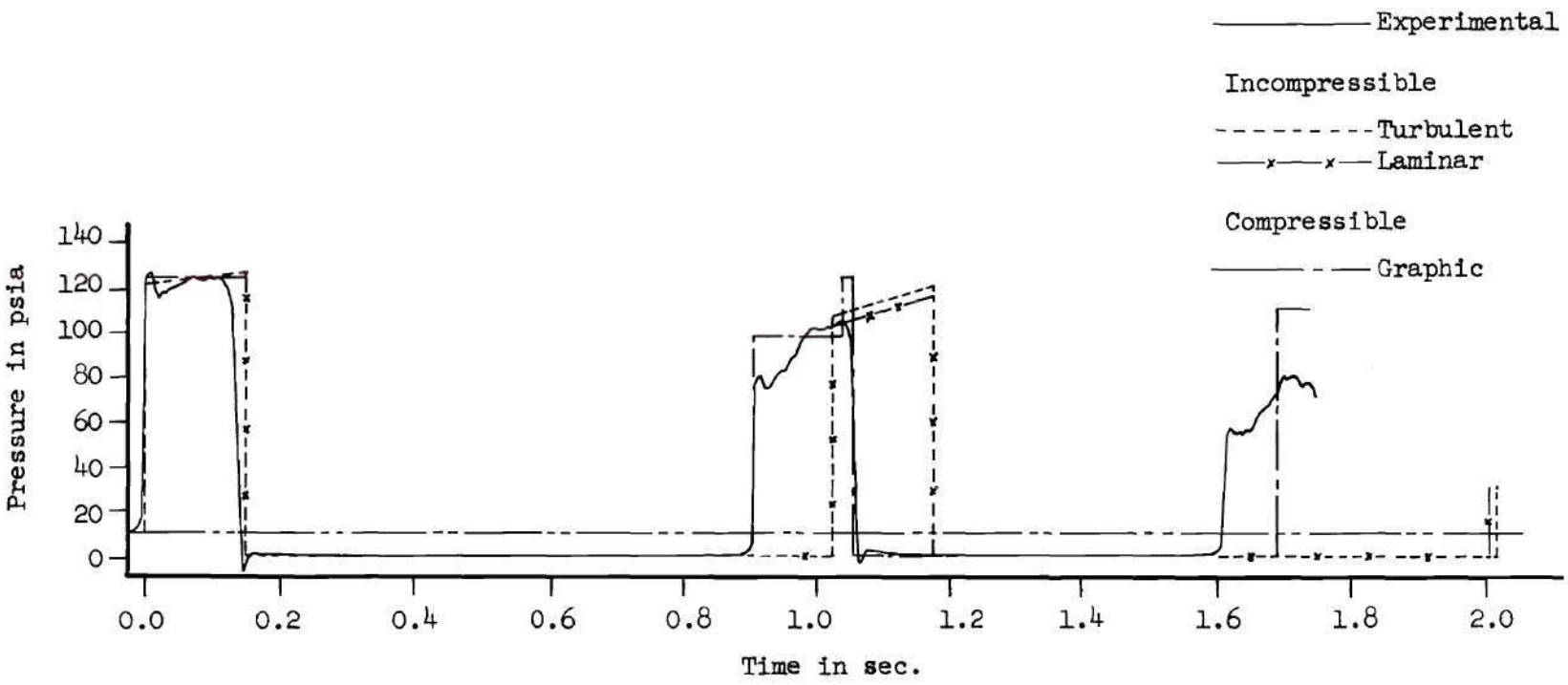

Figure 16. Experimental and Theoretical Results: Run 5

were traced from the original recorder data. The results of both incompressible-flow theories and also the compressible-flow solutions are superimposed on the experimental results.

In general, there is good correlation between the theoretical and experimental results for the first positive wave. In all cases where a discrepancy existed, the theoretical pressure was greater than the experimental pressure. The greatest deviation occurred in Run 2 (Fig. 13), where the difference was 1.9 per cent. It is felt that these results are an excellent confirmation of theory for the first positive wave.

The incompressible-flow equations do not accurately predict either the time of vapor cavity existence or the magnitude of the positive waves following the collapse of the cavity. It can be seen in Fig. 12 through 16 that for both incompressible-flow theories the calculated times of vapor cavity existence are almost equal. Since the resistence is considerably greater for laminar flow than for turbulent flow, it is concluded that the time of cavity existence is only slightly affected by pipe friction.

The pressure magnitude following the collapse of the vapor cavity is somewhat affected by the resistance of the pipe in the incompressible analyses. The greater friction of laminar flow gives rise to compression waves of smaller magnitude than those computed for turbulent flow. For the second shock wave, the variation of the laminar analysis with the experimental results was from 1.8 per cent in Run 4 to 18 per cent in Run 2. The variation between the laminar and turbulent analyses was from 1.4 per cent in Run 4, in which the magnitude of the turbulent

pressure rise was less than the magnitude of the laminar pressure rise, to 5 per cent in Runs 1 and 5, in which the turbulent pressure rise was greater than the laminar pressure rise.

The results of the compressible-flow (graphic) analysis show much better correlation with the experimental results than do the incompressible-flow analyses. It is difficult to make a quantitative comparison of the magnitudes of pressure rise on account of the stepped construction obtained by the graphic procedure. It is thought that because of the frequency of response of the transducer some of the pressure fluctuations of short duration may not have been recorded. However, it can be seen in Fig. 12 through 16 that except for these short-term pressure rises, the results agree closely. In Runs 3 and 5 there was no discrepancy between experimental and theoretical times for the first cavity. The greatest variation occurred in Run 1, where the experimental time was 6.3 per cent greater than the theoretical time. For the second cavity, the greatest time variation came in Run 2, where the difference was 19 per cent.

From the examination of results, it can be seen that the elastic-wave analysis gives much better agreement with experimental results than do the incompressible-flow analyses. It is believed that the time of vapor cavity existence is a factor in determining which method of analysis should be used. For the system under investigation, the time of vapor cavity existence is about five times greater than $2L/c$. For a much greater time of cavity existence, say greater than ten times $2L/c$, it is possible that an incompressible-flow analysis would be applicable. For times less than ten times $2L/c$, the elastic-wave analysis should be used.

CHAPTER VI

CONCLUSIONS AND RECOMMENDATIONS

Conclusions

1. Classic theory of water-hammer is accurate within one per cent of experimental results for the first compression shock-wave following rapid closure of a downstream valve in a pipe.

2. In systems with low steady-flow pressure at the valve, a vapor cavity forms upstream from the valve following the return of the shock-wave to the valve. This vapor cavity exists for several times longer than the time for the compression wave to make the round trip from the valve to the reservoir.

3. Pipe resistance has little effect on the time of vapor-cavity existence. However, as friction increases in the pipe, the magnitude of the pressure rise following collapse of the vapor-cavity decreases.

4. In systems in which the time of vapor-cavity existence is less than ten times $2L/c$, incompressible-flow theory does not accurately predict the experimental results. In such cases, the problem must be analyzed by compressible-flow theory.

Recommendations

1. A short section of transparent tubing should be installed in the present experimental apparatus so that the vapor cavity can be studied visually.

2. If possible, a system should be constructed in which the vapor cavity would exist for about 10 to 15 times $2L/c$. Further comparisons of incompressible-flow and compressible-flow analyses could then be made.

LITERATURE CITED

1. Leconte, Joseph N., "Experiments and Calculations on the Resurge Phase of Water-Hammer," Transactions of the American Society of Mechanical Engineers, Vol. 59, 1937, pp.691-694.

2. Bergeron, L., Water-Hammer in Hydraulics and Wave Surges in Electricity (translated from the French by a committee from the American Society of Mechanical Engineers), New York: John Wiley and Sons, Inc., 1961, pp. 80-84.

3. McNown, J. S., "Surges and Water-Hammer," Chapter 7 of Engineering Hydraulics, edited by H. Rouse, New York: John Wiley and Sons, Inc., 1950, pp. 468-495.

4. Carslaw, H. S., and J. C. Jaeger, Conduction of Heat in Solids, Second ed., Oxford: Claredon Press, 1959, pp. 188 and 201, 202.

OTHER REFERENCES

5. Parmakian, John, Water-Hammer Analysis, New York: Prentice-Hall, 1955.

6. Kephart, J. T., and Kenneth Davis, "Pressure Surges Following Water-Column Separation," Transactions of the American Society of Mechanical Engineers, Vol. 83, 1961, pp.456-460.

7. Richards, R. T., "Water-Column Separation in Pump Discharge Lines," Transactions of the American Society of Mechanical Engineers, Vol. 78, 1956, pp. 1297-1304.

8. de Haller, P., and A. Bedne, "Break-Away of Water Columns as a Result of Negative Pressure Shocks," Sulzer Technical Review, Vol. 4, 1951, pp. 18-25.

9. Duc, J., "Negative Pressure Phenomena in a Pump Pipe Line," Sulzer Technical Review, Vol. 41, 1959, pp. 3-11.

10. Charmonmon, S., Unpublished Report of the SEATO Graduate School Hydraulics Laboratory, 1960.